Latent Fingerprint Matching: Performance Gain via Feedback from Exemplar Prints

Sunpreet S. Arora, *Student Member, IEEE*, Eryun Liu, *Member, IEEE*, Kai Cao, and Anil K. Jain, *Fellow, IEEE*

Abstract—Latent fingerprints serve as an important source of forensic evidence in a court of law. Automatic matching of latent fingerprints to rolled/plain (exemplar) fingerprints with high accuracy is quite vital for such applications. However, latent impressions are typically of poor quality with complex background noise which makes feature extraction and matching of latents a significantly challenging problem. We propose incorporating top-down information or feedback from an exemplar to refine the features extracted from a latent for improving latent matching accuracy. The refined latent features (e.g. ridge orientation and frequency), after feedback, are used to re-match the latent to the top K candidate exemplars returned by the baseline matcher and resort the candidate list. The contributions of this research include: (i) devising systemic ways to use information in exemplars for latent feature refinement, (ii) developing a feedback paradigm which can be wrapped around any latent matcher for improving its matching performance, and (iii) determining when feedback is actually necessary to improve latent matching accuracy. Experimental results show that integrating the proposed feedback paradigm with a state-of-the-art latent matcher improves its identification accuracy by 0.5-3.5 percent for NIST SD27 and WVU latent databases against a background database of 100k exemplars.

Index Terms—Fingerprint, latent fingerprint matching, exemplar feedback, feature refinement, candidate list

1 Introduction

Sir Francis Galton first conceived the notion of uniqueness and individuality of the friction ridge patterns present on the palms of our hands and soles of our feet in the year 1892 [1]. Ever since, fingerprints have been widely used to determine the identity of an individual or to verify his claimed identity in both civilian and law enforcement applications. Law enforcement agencies, in particular, have used fingerprints for identifying suspects since the late 19th century [2]. The identification division of the Federal Bureau of Investigation (FBI), for instance, was established in 1924, and it currently has fingerprints of more than 70 million subjects, including more than 34 million civilian subjects, on record [3].

Based on the acquisition process, fingerprints can be broadly categorized into one of the following three types, (i) *rolled fingerprints* which contain almost all of the ridge details and are captured by rolling a finger from nail-to-nail, (ii) *plain/slap fingerprints* which are acquired by pressing the finger on a flat surface, and (iii) *latent fingerprints*[1] which are partial impressions of the finger inadvertently left behind on the surface of objects when they are touched or handled. They are either captured photographically or lifted from objects using complex chemical or physical methods [2], [4]. Latent prints, in particular, are of critical value in forensic applications because they are usually encountered at crime scenes and serve as a crucial evidence in a court of law.

Rolled and plain impressions (collectively called exemplars[2]), in general, are good quality fingerprints acquired under expert supervision either at the time of enrollment or booking (of suspects). They usually contain sufficient amount of discriminatory ridge valley patterns, minimal background noise and minor non-linear distortions. Because they are of reasonably good quality, exemplars can be automatically matched to each other with a high degree of accuracy. The best performing commercial matcher in the Fingerprint Vendor Technology Evaluation (FpVTE) [5] conducted by the National Institute of Standards and Technology (NIST) achieved rank-1 identification rate of 99.4 percent on a database of 10,000 plain fingerprint images.

Latent fingerprints, on the other hand, are partial impressions of the finger, and thus have relatively smaller area containing friction ridge patterns. They generally exhibit poor quality in terms of ridge clarity due to the

- *S.S. Arora and A.K. Jain are with the Department of Computer Science and Engineering, Michigan State University, East Lansing, MI 48824. E-mail: {arorasun, jain}@cse.msu.edu.*
- *E. Liu is with the Department of Information Science & Electronic Engineering, Zhejiang University, Hangzhou, Zhejiang 310027, China. E-mail: eryunliu@zju.edu.cn.*
- *K. Cao is with the Department of Computer Science and Engineering, Michigan State University, East Lansing, MI 48824, and the School of Life Sciences and Technology, Xidian University, Xi'an, Shaanxi 710126, China. E-mail: kaicao@cse.msu.edu.*

Manuscript received 27 Dec. 2013; revised 11 May 2014; accepted 3 June 2014. Date of publication 11 June 2014; date of current version 5 Nov. 2014. Recommended for acceptance by D. Maltoni.
For information on obtaining reprints of this article, please send e-mail to: reprints@ieee.org, and reference the Digital Object Identifier below.
Digital Object Identifier no. 10.1109/TPAMI.2014.2330609

1. The term *fingermark* is commonly used in the forensics community to refer to an impression of a finger left behind on a surface and is more appropriate as not all fingermarks are latents. However, we use the term *latent fingerprint* here which is more popular in the biometrics community for such impressions, and is more relevant in the context of this research.

2. The term *exemplar* is used to refer to the rolled/plain fingerprints in the background or reference database.

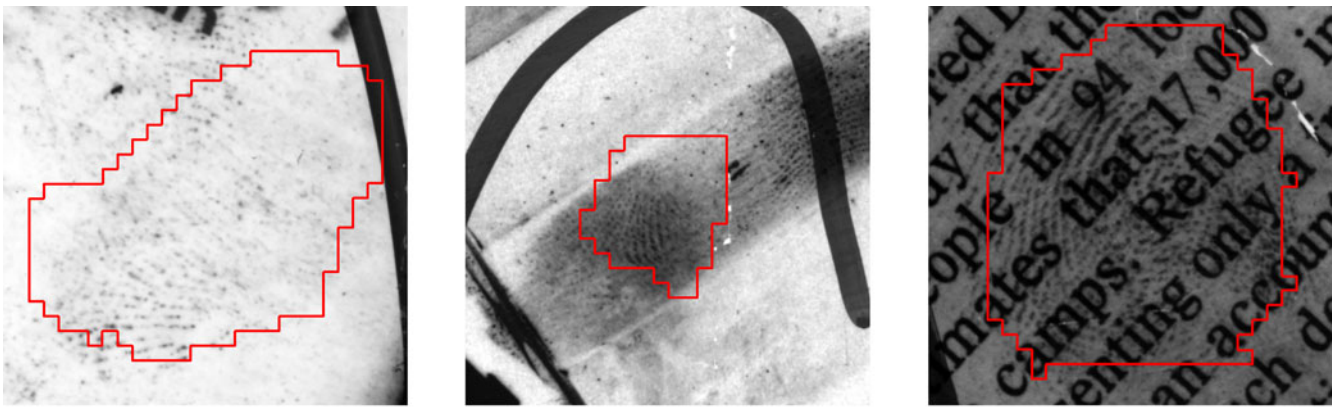

Fig. 1. Sample images from the NIST SD27 database shown here to elucidate some of the challenges in latent fingerprint matching: (a) poor ridge clarity, (b) insufficient amount of usable ridge valley patterns and (c) presence of complex background noise. The red curves are manually marked foreground area in the image.

presence of complex background noise (Fig. 1), and have large non-linear distortions due to variations in finger pressure when an object is touched, resulting in the print on its surface. Automatically matching latent fingerprints to exemplars is, therefore, significantly more challenging. In the Evaluation of Latent Fingerprint Technologies (ELFT) [6] conducted by NIST, the Phase-I results showed that the best rank-1 latent identification accuracy was 80 percent in identifying 100 latent images from amongst a set of 10,000 rolled prints [7]. More recently, in the NIST Evaluation of Latent Fingerprint Technologies: Extended Feature Sets (ELFT EFS) Phase II [8], the rank-1 identification accuracy of the best performing latent matcher was only 63.4 percent in the "lights-out" (fully automatic) identification mode.[3]

To summarize, while the Automated Fingerprint Identification Systems (AFIS) work extremely well in matching exemplar fingerprints to each other, there is a considerable performance drop when matching latent fingerprint images to exemplar images. It is generally agreed that latent fingerprint matching is a challenging problem whose performance needs to be significantly improved to reduce the backlog of operational cases in law enforcement agencies. The FBI's Next Generation Identification (NGI) program [9] lists "lights-out" capability for latent identification as one of its major objectives.

In manual matching of latent prints, latent fingerprint examiners usually follow the *Analysis, Comparison, Evaluation and Verification* (ACE-V) methodology [10]. This basically, is a four step process:

1) *Analysis*. The preliminary step involves analyzing the latent image to ascertain if the latent is of sufficient value for processing and manually marking features such as minutiae, orientation field and ridge frequency. This is usually done by observing the latent image in isolation.
2) *Comparison*. This consists of comparing the latent image to the exemplar image in terms of their features, and assessing the degree of similarity/dissimilarity between latent and exemplar.
3) *Evaluation*. The latent examiner determines the strength of the evidence between the latent and exemplar based on the assessed degree of similarity/dissimilarity between the latent and exemplar in the comparison step.
4) *Verification*. A second latent examiner independently evaluates the latent-exemplar pair to validate the results of the first latent examiner.

The ACE-V procedure is a tedious and time consuming process for the latent examiner as it may involve a large number of fingerprint comparisons between different exemplar fingerprint pairs. For this reason, AFIS is used in the comparison step. Typically, a list of top K matching candidates (with K generally being 50) is retrieved from the exemplar fingerprint database using a latent matcher, which are then visually inspected by the latent examiner to ascertain the best match. This results in one of the following five outcomes:

1) The latent examiner correctly matches the latent fingerprint to its true mated exemplar from the candidate list.
2) The examiner erroneously matches the latent fingerprint to an exemplar fingerprint from the candidate list (which is not the true mate).
3) The examiner correctly excludes an exemplar fingerprint from the candidate list (which is not the true mate) to be the possible mate of the latent fingerprint.
4) The examiner erroneously excludes the true mated exemplar fingerprint of the latent fingerprint from the candidate list to be the possible mate of the latent.
5) The examiner deems the matching result to be inconclusive because he is unable to find any candidate exemplar that is sufficiently similar to the latent print.

Note that while outcome 2) is an erroneous match and outcome 4) an erroneous exclusion, outcome 5) is a reject in the sense that the true mate does not exist in the background database. The proposed feedback based methodology is

3. The latent matching accuracy is significantly higher in the ELFT Phase-I as compared to Phase-II because the quality of latents used in Phase-I evaluation was comparatively better.

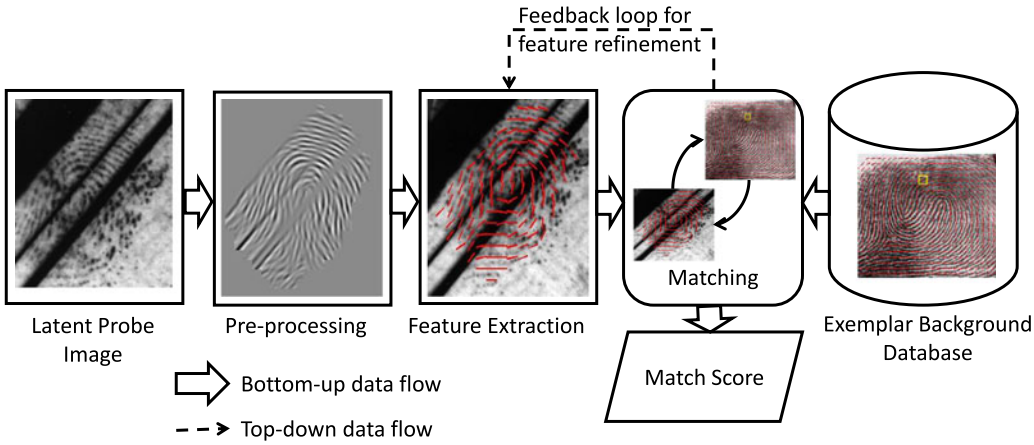

Fig. 2. Illustrating the typical bottom-up data flow used in latent to exemplar matching systems. The dotted line shows the feedback path (top-down data flow) in the proposed matching paradigm.

designed to minimize the occurrence of outcomes 2), 4) and 5) by initially retrieving a much larger candidate list (e.g., $N = 200$) using the AFIS. Each of these candidates is then viewed as the output of a coarse level match which can be used to refine the features extracted from the latent images. The similarities of these N candidates to the query latent are then recomputed based on the refined latent features to re-rank the candidate list. The latent examiner can then examine the top K candidates ($K < N$) from this re-ranked list for determining the strength of evidence between the latent and candidate exemplars during the evaluation step.

State-of-the-art latent matching systems [11], [12], [13], [14] are based on the classical bottom-up matching strategy [15]. The bottom-up approach basically builds a system from several sub-systems or components. In essence, there is a sequential "bottom-up" data flow from preprocessing and feature extraction to matching and match score computation. However, the basic assumption in bottom-up systems is that if all the individual sub-systems are functioning well, the system as a whole would function well too [16]. In our opinion, this assumption does not hold good for latent matching systems because the feature extraction sub-system does not work sufficiently well for extracting features from operational latents due to the presence of different kinds of structural noise in the latent image [17].

On the other hand, the importance of a feedback mechanism between components or the "top-down" data flow is well known [15]. Bottom-up and top-down approaches have been widely used to model human perception system in cognitive science [18]. Oliver et al. [19] used these strategies to develop a computer vision system for recognizing and modeling human interactions. Top-down approaches or feedback mechanisms have been used for object detection and segmentation [20], [21] and for improving the decision making capabilities of artificial neural networks [22].

In this paper, we extend this idea of feedback to latent fingerprint matching by incorporating a top-down data flow between the matching module and feature extraction module (see the dotted line in Fig. 2). We devise systemic ways to use information in exemplars for refining latent features, e.g., ridge orientation and frequency, and use them to develop a feedback paradigm which could be integrated into a latent matcher to improve its matching accuracy. Note that there is a difference between the feedback approach used in manual latent matching [23] and the idea of using feedback from exemplars for refining latent features proposed in this paper. In manual latent matching, the top-down information usually refers to the prior training, bias and the state of mind of latent examiners which may influence the outcome of latent examination. The proposed paradigm, however, uses feedback in the matching stage to refine the features extracted from the latent images. This feedback is particularly useful because features extracted from the latent are often unreliable due to their poor quality. In our opinion, matching latent images based on the initially extracted set of features without any prior information (bottom-up mode) is prone to error. Additional top-down information flow provided by feedback allows the matching system to use the hypothesized exemplar mate to refine initially extracted features from the latent and improve the matching accuracy.

Nevertheless, there are cases when the latent image is of good quality and reliable features can be extracted in the bottom-up mode, making feedback unnecessary. To determine if feedback is indeed needed for a latent query, we devise a global criterion based on the match score probability distribution obtained by matching the latent to the top K candidate exemplars. For determining the regions within the latent image which need feedback as well the regions of the exemplar which are of sufficiently good quality to provide feedback, we use a local fingerprint quality metric.

To demonstrate the effectiveness of the proposed feedback based latent matching strategy, we integrate the feedback paradigm with a state-of-the-art latent matcher [14] and conduct experiments on two different latent databases (NIST SD27 [24] and WVU [25]). A marked improvement in matching accuracies is observed when using feedback from exemplars in the latent matching process. Besides, there is only one latent query for which feedback is not provided when it could have been useful. This demonstrates the efficacy of the proposed criterion to decide if feedback is needed for a latent query.

2 Feedback Paradigm for Latent Matching

Let I^L be the latent probe image and I^R be an exemplar image from the background database. Let Θ be the set of

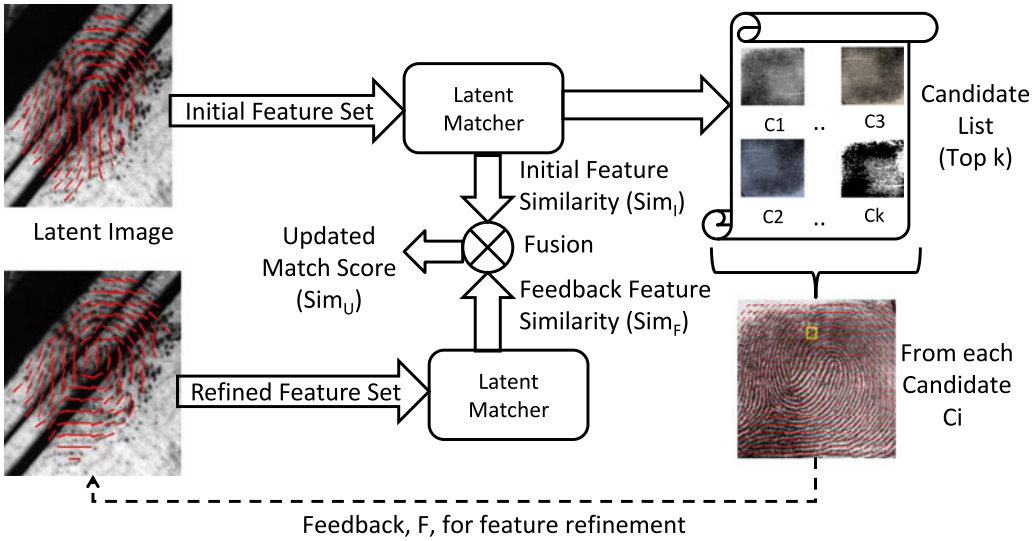

Fig. 3. Resorting the candidate list using feedback. Note the refinement of latent features due to feedback.

features extracted from the fingerprint image. Here we denote the feature set corresponding to the latent by Θ^L and that of the exemplar image by Θ^R. Typically, feature set Θ^R is pre-computed for each exemplar image. The bottom-up matching process involves matching the two representations Θ^L and Θ^R and assigning the initial match score Sim_I:

$$Sim_I = S_I(\Theta^L, \Theta^R). \tag{1}$$

Here S_I is the similarity function used to generate the match score between the latent fingerprint feature set Θ^L and the exemplar feature set Θ^R.

The top K candidate exemplars based on these similarities are retrieved from the background database. Feedback is then provided from the feature set Θ^R of the candidate exemplar image to refine the feature set Θ^L initially computed from the latent image. The refined feature set denoted by $\hat{\Theta}^L$ is computed using a function f of the initial feature set Θ^L and the feedback information F as follows:

$$\hat{\Theta}^L = f(\Theta^L, F). \tag{2}$$

The feedback feature similarity Sim_F between $\hat{\Theta}^L$ and Θ^R is then computed using the similarity function S_F as follows:

$$Sim_F = S_F(\hat{\Theta}^L, \Theta^R). \tag{3}$$

Finally, the updated match score Sim_U is calculated from Sim_I and Sim_F using a match score fusion operator $\otimes$:

$$Sim_U = Sim_I \otimes Sim_F. \tag{4}$$

3 Resorting Candidate List Based on Feedback

The feedback based paradigm is applied for resorting the candidate list of top K candidate exemplars retrieved by a state-of-the-art latent matcher [14] (see Fig. 3). The matcher in [14] is chosen because it is one of the best performing available latent matchers[4] using minimal human input (requires only marked minutiae for latents). This matcher is referred to as the *baseline matcher* henceforth because it is used to match a latent to the exemplar background database to generate the candidate list.

The feedback implementation broadly consists of the following four steps (see Fig. 4):

1) *Initial matching and alignment*. The baseline matcher is used to obtain the initial match score, and to generate the minutiae correspondences between an input latent and an exemplar image. The latent is then aligned to the exemplar image using the scaling, rotation and translation parameters estimated based on the minutiae correspondences.
2) *Exemplar feature extraction*. Exemplar image is divided into blocks of size 16 by 16. Ridge orientation and frequency features are extracted within each block of the exemplar.
3) *Latent feature extraction and refinement*. Latent image is divided into blocks of size 16 by 16. For each block in the latent, ridge orientation and frequency features corresponding to peak points in the magnitude spectrum of the frequency domain are extracted. The extracted features within each block are then refined based on the feedback from features extracted in the corresponding exemplar block. Feedback consists of orientation differences between each extracted ridge orientation in the latent block and the ridge orientation in the corresponding exemplar block.
4) *Match score computation*. The similarity between the refined latent features and the exemplar features is used to compute an updated match score between the latent and the exemplar.

4. While we have access to a commercial latent SDK, we were not able to use it in our experiments because the SDK does not output minutiae correspondences between latent and exemplar. While some of the commercial tenprint SDKs, such as Verifinger by Neurotechnology (http://www.neurotechnology.com/verifinger.html), provide minutiae correspondence, they do not perform well for latent to exemplar matching since they were not designed for this scenario.

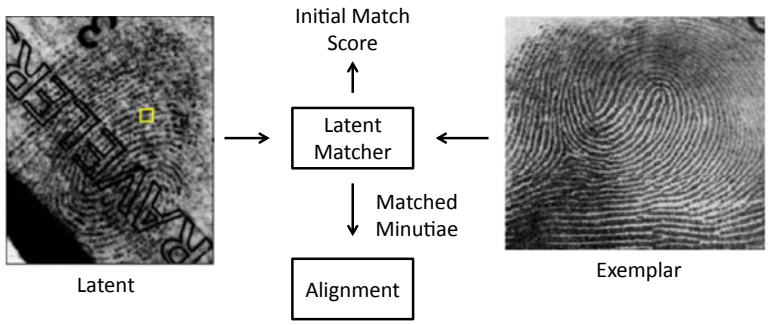

(a) Initial Matching and Alignment

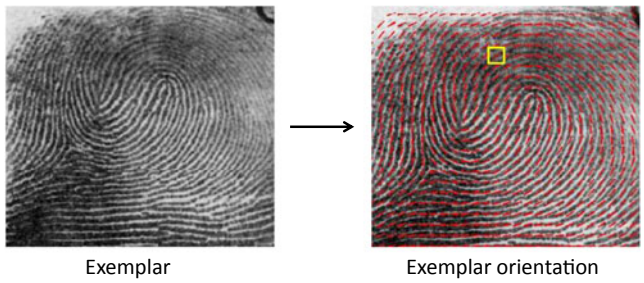

(b) Exemplar Feature Extraction

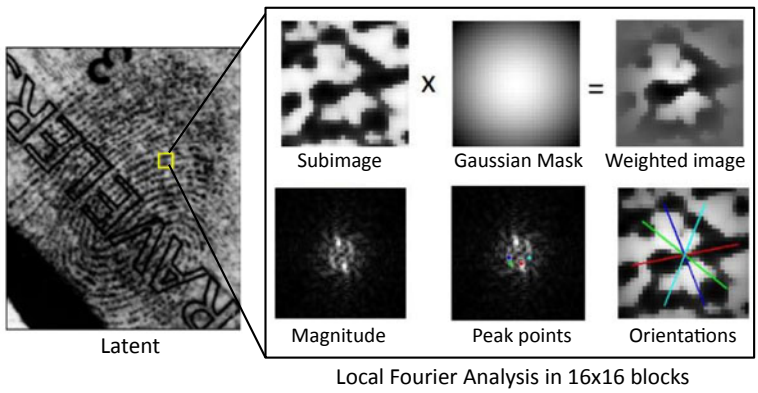

(c) Latent Feature Extraction

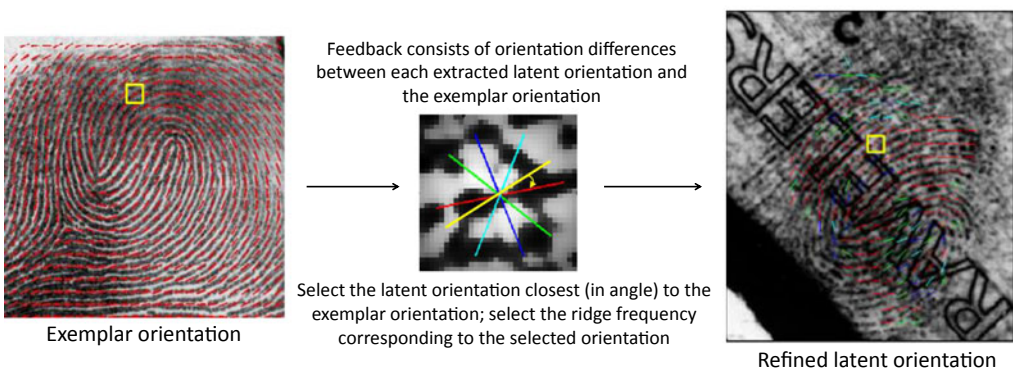

(d) LatentFeatureRefinement

Fig. 4. Major steps involved in latent fingerprint matching using feedback from exemplar. The refined latent features illustrated in (d) are used to rematch the latent to the exemplar and resort the candidate list. Shown in yellow is a pair of corresponding latent and exemplar blocks.

The candidate list is resorted based on the updated match scores between the latent and the retrieved exemplars returned by the baseline matcher.

3.1 Initial Matching and Alignment

Manually marked minutiae in the latent image and automatically extracted minutiae from the exemplar image

(using a commercial off-the-shelf (COTS) matcher) are fed as input to the baseline matcher to obtain the initial match score Sim_I and a list of matched minutiae.[5] Let $M^L = \{(x_i^L, y_i^L, \theta_i^L) | i = 1, 2, \ldots, P\}$ represent the list of matched minutiae for the latent and $M^R = \{(x_i^R, y_i^R, \theta_i^R) \,|\, i = 1, 2, \ldots, P\}$ represent the list of corresponding matched minutiae for the exemplar, where (x, y) are the coordinate values, θ is the direction of minutia and P is the number of matched minutiae pairs.

Depending on the number of matched minutiae pairs P, the transformation T for aligning the latent to the exemplar is estimated differently:

Case I ($P \geq 2$). The transformation $T(x, y; a, b, t_x, t_y)$ is estimated by solving the following set of equations:

$$\begin{bmatrix} x_i^R \\ y_i^R \end{bmatrix} = \begin{bmatrix} a & -b \\ b & a \end{bmatrix} \begin{bmatrix} x_i^L \\ y_i^L \end{bmatrix} + \begin{bmatrix} t_x \\ t_y \end{bmatrix}, i = 1, 2, \ldots, P. \quad (5)$$

Here, $a = s \cos \Delta\theta$ and $b = s \sin \Delta\theta$, where s is the scale parameter and $\Delta\theta$ is the rotation angle, and t_x and t_y are the translation parameters. This system of linear equations can be solved by minimizing the least square error.

Now, given the coordinates (x^L, y^L) of any point in the latent image, its transformed coordinates (x^R, y^R) in the exemplar coordinate system can be obtained by using the transformation T:

$$\begin{bmatrix} x^R \\ y^R \end{bmatrix} = \begin{bmatrix} a & -b \\ b & a \end{bmatrix} \begin{bmatrix} x^L \\ y^L \end{bmatrix} + \begin{bmatrix} t_x \\ t_y \end{bmatrix}. \quad (6)$$

Case II ($P = 1$). If only one pair of matched minutiae is available, the transformation function is estimated by utilizing both the minutiae location and direction. Let $(x_1^L, y_1^L, \theta_1^L)$ and $(x_1^R, y_1^R, \theta_1^R)$ be the matching pair of minutiae in the latent and exemplar, respectively. The rotation angle from latent to exemplar is then estimated by:

$$\Delta\theta = \theta_1^R - \theta_1^L. \quad (7)$$

Given a point (x^L, y^L) in the latent, its transformed coordinates (x^R, y^R) in the exemplar coordinate system can be calculated by using the transformation T:

$$\begin{bmatrix} x^R \\ y^R \end{bmatrix} = \begin{bmatrix} \cos \Delta\theta & -\sin \Delta\theta \\ \sin \Delta\theta & \cos \Delta\theta \end{bmatrix} \begin{bmatrix} x^L - x_1^L \\ y^L - y_1^L \end{bmatrix} + \begin{bmatrix} x_1^R \\ y_1^R \end{bmatrix}. \quad (8)$$

Note that this transformation does not include any scaling factor because it cannot be estimated based on just a single pair of matched minutiae.

To summarize, translation, scaling and rotation parameters for aligning the latent and the exemplar are estimated based on the matched minutiae pairs. The transformation is then used to align the two images.

5. Feeding the baseline matcher used in our experiment with automatically extracted minutiae from latents either does not generate any minutiae correspondences or generates a number of false minutiae correspondences. This degrades the alignment of the latent-exemplar pair and results in improper feedback. However, this paradigm can be used in the "lights-out" identification mode, provided the baseline matcher does not produce many false minutiae correspondences and the latent-exemplar pair can be well aligned.

3.2 Exemplar Feature Extraction

Two different types of local features are computed for the exemplar image, namely ridge orientation and ridge frequency. Given an exemplar image I^R, its ridge skeleton image I_{sk}^R is first extracted using a COTS matcher. The skeleton image is then divided into 16 by 16 pixel blocks. Ridge orientation and ridge frequency are then computed for each block I_B^R in the skeleton image I_{sk}^R.

3.3 Latent Feature Extraction and Refinement

The level one features (e.g., ridge orientation and ridge frequency) in the latent image are difficult to extract because of the presence of structured noise in the background. Local Fourier analysis is used for this purpose because it has been shown to be resilient to complex background noise [26], [13].

Similar to the exemplar image, the latent image I^L is first divided into 16 by 16 blocks. For each block I_B^L in the region of interest (ROI) of the latent, the local ridge orientation and ridge frequency features are obtained as follows:

1) A 32×32 sub-image $I_{B'}^L$ centered at the block I_B^L is extracted and convolved with a Gaussian filter of the same size with $\sigma = 16$.
2) The sub-image $I_{B'}^L$ is padded with zeros on the borders to get a 64×64 image $I_{B''}^L$. This is done to increase the number of sampling points in the discrete Fourier domain.
3) Fast Fourier Transform (FFT) is applied to the padded sub-image $I_{B''}^L$. For each peak (u, v) in the magnitude spectrum image, the corresponding orientation α and frequency f is computed by:

$$\alpha^L = \arctan\left(\frac{u}{v}\right), \quad (9)$$

$$f^L = \sqrt{(u^2 + v^2)}/64. \quad (10)$$

4) A set of L peak points $H = \{(u_i, v_i) \,|\, i = 1, 2, \ldots, L\}$ of highest magnitude values, and with frequency value satisfying $\frac{1}{16} < f < \frac{13}{64}$, is selected. Note that L is set to 4 in our implementation.
5) The (x, y) coordinates of the central pixel in the block I_B^L are then transformed to the exemplar coordinate system using the transformation function T estimated previously. Let the transformed coordinates of that pixel be represented as (x', y').
6) Let α^R be the corresponding ridge orientation of the block containing the pixel (x', y') in the exemplar image. The peak point l (from the set H) corresponding to the closest ridge orientation to α^R from amongst the ridge orientations α_i^L, is then selected as follows:

$$l = \arg \min_i \varphi\left(\alpha_i^L + \Delta\theta, \alpha^R\right), \quad (11)$$

where $1 \leq i \leq L$ and

$$\varphi(\alpha, \beta) = \begin{cases} |\alpha - \beta|, \text{if } |\alpha - \beta| < 90, \\ 180 - |\alpha - \beta|, \text{otherwise.} \end{cases} \quad (12)$$

Here, $\varphi(\alpha, \beta)$ is the function to determine the difference between ridge orientations α and β and $\Delta\theta$ is the rotation angle used to align the two ridge orientations α and β.

7) The ridge orientation and ridge frequency values corresponding to the selected peak point (u_l, v_l) are then chosen as the refined ridge orientation and ridge frequency features for the block I_B^L in latent image.

Note that the refined ridge orientation and ridge frequency features are selected based on the exemplar features, and this essentially constitutes the top-down information flow or feedback from the exemplar.

3.4 Match Score Computation

The functions to compute the similarity between the exemplar features and the refined latent features after feedback should result in improved similarity between mated latent-exemplar pairs. Thus, the similarity function should be based on the underlying distribution of feature differences obtained from genuine latent-exemplar matches. Assume that the orientation and frequency differences between the refined latent features and exemplar features within each block are independent and identically distributed (i.i.d). To learn the characteristics of the genuine distribution model, 50 mated latent-exemplar pairs from the NIST SD27 [24] and WVU database [25] are randomly sampled to estimate the distributions. We observe that the genuine distribution of orientation differences approximately follows a cosine curve whereas that of ridge frequency differences approximates an exponential curve; cosine and exponential functions are hence used for computing feedback orientation and frequency similarities, respectively.

For computing the feedback ridge orientation and frequency similarities, the overlapping region between the latent and exemplar is first determined using the transformation function T. Within the overlapping region, the ridge orientation and ridge frequency similarities Sim_α and Sim_f are then computed as:

$$Sim_\alpha = \frac{1}{Num}\sum_{i=1}^{Num} \cos\left(-\frac{\varphi\left(\alpha_i^L + \Delta\theta, \alpha_i^R\right)}{\mu_\alpha}\right), \tag{13}$$

$$Sim_f = \frac{1}{Num}\sum_{i=1}^{Num} \exp\left(-\frac{\left|\frac{1}{f_i^L} - \frac{1}{f_i^R}\right|}{\mu_f}\right), \tag{14}$$

$$Num \geq Num_{min},$$

where Num is the number of overlapping blocks; Num_{min} is a threshold on the minimum number of blocks needed in the overlapping region and is set to 10 in our experiments; α_i^L and α_i^R are the ridge orientations and f_i^L and f_i^R are the ridge frequencies of the ith overlapping block from the latent and exemplar, respectively; μ_α and μ_f are two normalization parameters which are empirically set to 12 and 8, respectively. The initial match score Sim_I is first normalized using min-max score normalization [27], and the orientation and frequency similarities Sim_α and Sim_f are then combined with the normalized initial match score Sim_{NI} based on product fusion to obtain the updated match score Sim_U as follows:

$$Sim_U = Sim_{NI} \times Sim_\alpha \times Sim_f. \tag{15}$$

4 The Adequacy of Feedback

Although feedback from exemplars can be used to refine latent features, the feedback may not be necessary when the latent is of sufficient good quality such that its features can be reliably extracted. Bottom-up latent to exemplar matching may suffice for such cases and feedback may not add any value to the latent matching process. Clearly, it would be useful to have an objective criterion to ascertain if feedback can potentially improve the matching accuracy for each latent query. Besides, since feedback is applied within each block in the latent, decision to apply feedback can also be made locally at the block level. To determine the need for feedback, we design a *global criterion* based on the match score distribution (of the top K match scores returned by the baseline latent matcher), and a *local criterion* based on the local quality of the latent-exemplar pair being matched.

4.1 Global Criterion

We design a simple criterion to decide whether feedback is needed for a particular latent query based on the probability distribution of the top K match scores returned by the baseline matcher.

4.1.1 Modelling the Match Score Distribution

This distribution is based on the similarity function used in the baseline matcher. The latent matcher used in our experiments [14] uses an exponential similarity function, so we use the exponential distribution to model the probability distribution of match scores. Alternately, we could estimate the probability densities using the match score histogram, and then fit a parametric distribution to the histogram. To measure the goodness of fit of the exponential distribution model in our case, we used the chi-square goodness of fit test [28]. For this, we randomly sampled 40 latent images from the NIST SD27 database [24], and then tested the goodness of fit of the exponential distribution on the set of top K match scores generated by the matcher for each latent.

4.1.2 Test for the Presence of an Upper Outlier

We observe that if the true mated exemplar print is indeed retrieved at rank-1 by the baseline latent matcher operating in bottom-up mode, then there is a sizeable difference between the rank-1 and other match scores. In other words, the rank-1 match score is an upper outlier in the probability distribution of the top K match scores. Thus, the problem of determining whether feedback is needed or not becomes equivalent to the problem of detecting whether an upper outlier exists in the match score distribution (see Fig. 5).

We now describe a hypothesis test for detecting the presence of an upper outlier for exponential density used here [29] and its usage in determining the need for feedback.

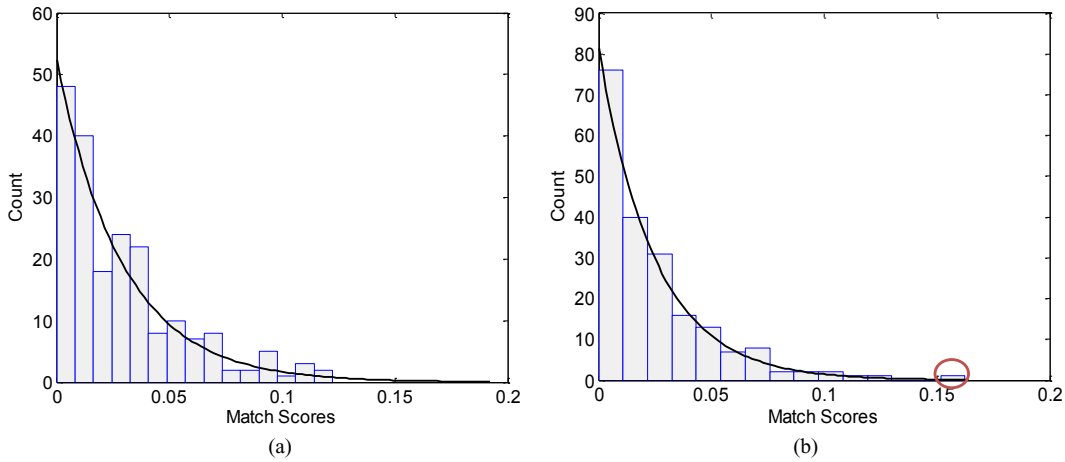

Fig. 5. Exemplifying the global criterion for feedback: (a) match score distribution for a particular latent query without an upper outlier, and (b) with an upper outlier present (marked in red). Feedback is needed in case (a), but not needed in (b).

The pdf of the exponential distribution with scale parameter λ is given by

$$f(x) = \frac{1}{\lambda} e^{-\frac{x}{\lambda}}; x > 0; \lambda > 0. \tag{16}$$

Let $X = \{X_1, X_2, \ldots, X_n\}$ be an independent and identically distributed (i.i.d) random sample of size n generated from an exponential distribution given by Eq. (16), and $X_{(1)}, X_{(2)}, \ldots, X_{(n)}$ be the corresponding order statistics. Order statistics are the sample values in the order of their magnitude with $X_{(1)} < X_{(2)} \cdots < X_{(n)}$. In our case, X pertains to the set of top K match scores, $X_{(1)}$ is the match score obtained by matching the latent to the Kth candidate exemplar, and $X_{(n)}$ is the match score generated on matching the latent to the 1st candidate exemplar.

To test for the upper outlier, the null hypothesis H_0 and the alternative hypothesis H_1 are defined as:

H_0. All observations in the set X are i.i.d from the exponential distribution.

H_1. Maximum match score is an upper outlier of the match score distribution.

The test statistic Z for testing the hypothesis is defined as:

$$Z = \frac{X_{(n)} - X_{(n-1)}}{S_n};\ S_n = \sum_{i=1}^{n} X_i. \tag{17}$$

To determine the critical value for the test, we obtain the distribution of the test statistic Z under the null hypothesis H_0. The sum S_n of n i.i.d. exponential random variables in the set X with a fixed scale parameter λ defined in Eqn. (17) follows a gamma distribution with shape parameter n and scale parameter λ [30]:

$$g(s, n, \lambda) = \frac{1}{\lambda^n} \frac{1}{\tau(n)} s^{n-1} e^{-\frac{s}{\lambda}}. \tag{18}$$

Here, $\tau(n)$ is the gamma function. The test statistic Z can be viewed as the difference of two random variables Z_1 and Z_2 where $Z_1 = X_{(n)}/S_n$ and $Z_2 = X_{(n-1)}/S_n$. Each of these random variables Z_1 and Z_2 follows a beta distribution with shape parameters 1 and $n-1$; the joint distribution of Z_1 and Z_2 [31] is then given by:

$$\begin{aligned} h(z_1, z_2) = n(n-1)(n-2)^2 \{ & (1 - z_1 - z_2)^{n-3}. \\ & - \binom{n-2}{1} (1 - z_1 - 2z_2)^{n-3} \\ & + \binom{n-2}{2} (1 - z_1 - 3z_2)^{n-3} \\ & - \cdots + (-1)^{t-1} \binom{n-2}{t-1} (1 - z_1 - tz_2)^{n-3} \}. \end{aligned} \tag{19}$$

Here $t = (1 - z_1)/z_2, (z_1 + z_2) < 1, z_1 + (n-1)z_2 > 1, z_1 > z_2$. Now, the density of Z can be computed using a bivariate transformation on the joint density of Z_1 and Z_2 [29] (Eq. (19)):

$$\begin{aligned} m(z) = \frac{n(n-1)^2}{n^{n-2}} \Bigg\{ & \frac{(n-2)^{n-2}}{2} - \binom{n-2}{1} \frac{(n-3)^{n-2}}{3} \\ & + \cdots + (-1)^{n-3} \binom{n-2}{n-3} \frac{1}{n-1} \Bigg\} (1 - z)^{n-2}. \end{aligned} \tag{20}$$

Here $0 < z < 1$. The probability of the test statistic Z being greater than the critical value $z(\alpha)$ at significance level α can be obtained from Eq. (20) as follows:

$$P[Z > z(\alpha) \mid H_0] = \int_{z(\alpha)}^{1} m(z) = (1 - z(\alpha))^{n-1} = \alpha. \tag{21}$$

Thus, the critical value $z(\alpha)$ is:

$$z(\alpha) = 1 - \alpha^{\frac{1}{n-1}}. \tag{22}$$

For $X_{(n)}$ to be the outlier, the realized value of the test statistic $Z = z$ should be greater than the critical value $z(\alpha)$. For the *global criterion* for feedback, we define an indicator random variable I_F which takes the value 1 when feedback is needed and 0, if it is not needed:

$$I_F = \begin{cases} 0, & z > z(\alpha), \\ 1, & \text{otherwise}. \end{cases} \tag{23}$$

4.2 Local Criterion

Even though feedback may be potentially useful for a particular latent query, there may be some good quality regions within the latent image which do not require feedback.

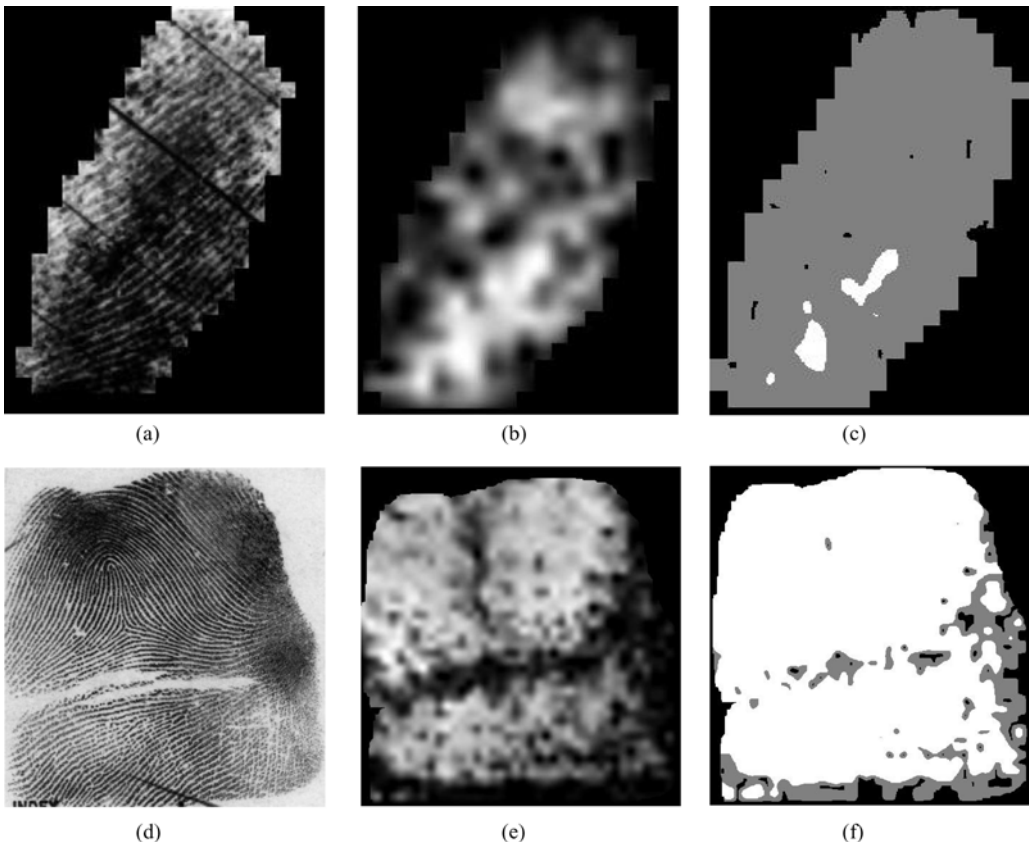

Fig. 6. Exemplifying the local criterion for feedback: (a) a latent image, (b) its ridge clarity map and (c) regions which need feedback (shown in grey); (d) an exemplar image, (e) its ridge clarity map and (f) regions which are reliable for providing feedback (shown in white).

Besides, the exemplar print region from where feedback is being taken may be of poor quality which may not be reliable for feedback. For deciding whether feedback is needed locally, we use the local fingerprint quality metric proposed in [32] called the *Ridge Clarity*. While this metric was proposed for latent images, we find that it is appropriate for estimating the local quality of exemplar fingerprints (Fig. 6).

The computation of ridge clarity for an image I involves the following four steps:

1) *Contrast enhancement*. Obtain the contrast-enhanced image I_C [33]:

$$I_C = sign(I - I_S) \times \log(1 + |I - I_S|). \tag{24}$$

Here, I_S is the image obtained using a 15×15 averaging filter on I, and $sign(x)$ is the signum function which outputs 1 if $x > 0$ and 0 otherwise.

2) *Frequency domain analysis*. The contrast-enhanced image I_C is divided into blocks of size 16×16, and a 32×32 subimage $I_C(x, y)$ is obtained around the center (x, y) of each block. $I_C(x, y)$ is then padded with zeros to obtain a 64×64 subimage $I_C^*(x, y)$. This subimage $I_C^*(x, y)$ is transformed into the frequency domain to obtain $F_C^*(s, t)$. Two peak points (s_1, t_1) and (s_2, t_2) corresponding to the two local amplitude maxima within frequency range $[0.0625, 0.2]$ in $F_C^*(s, t)$ are then selected [26]. The 2D sine wave $w_i(p, q)$ at the ith peak point in $F_C^*(s, t)$; $i = \{1, 2\}$ with amplitude a_i, frequency f_i, angle θ_i and phase ϕ_i is given by:

$$w_i(p, q) = a_i \sin(2\pi f_i(\cos(\theta_i)p + \sin(\theta_i)q) + \phi_i), \tag{25}$$

where

$$a_i = |F_C^*(s_i, t_i)|, f_i = \frac{\sqrt{s_i^2 + t_i^2}}{64},$$

$$\theta_i = \arctan\left(\frac{s_i}{t_i}\right), \phi_i = \arctan\left[\frac{Im(F_C^*(s_i, t_i))}{Re(F_C^*(s_i, t_i))}\right].$$

3) *Ridge continuity map computation*. Two neighbouring blocks b_1 and b_2 are said to be continuous if the following conditions hold for their corresponding sine waves bw_1 and bw_2:

$$\min\{|b\theta_1, b\theta_2|, \pi - |b\theta_1, b\theta_2|\} \leq T_{b\theta},$$

$$\left|\frac{1}{bf_1} - \frac{1}{bf_2}\right| \leq T_{bf},$$

$$\frac{1}{16}\sum_{\{p,q \in \psi\}}\left|\frac{bw_1(p, q)}{ba_1} - \frac{bw_2(p, q)}{ba_2}\right| \leq T_{bp}. \tag{26}$$

Here, $T_{b_\theta}, T_{bf}, T_{bp}$ are constants set to $\pi/10$, 3 and 0.6, respectively, and ψ refers to the set of 16 pixels which lie on the border of two neighbouring blocks. Define an indicator function I_{fc} for ridge continuity as:

$$I_{fc} = \begin{cases} 1, & sw_1 \text{ and } sw_2 \text{ are continuous,} \\ 0, & \text{otherwise.} \end{cases} \tag{27}$$

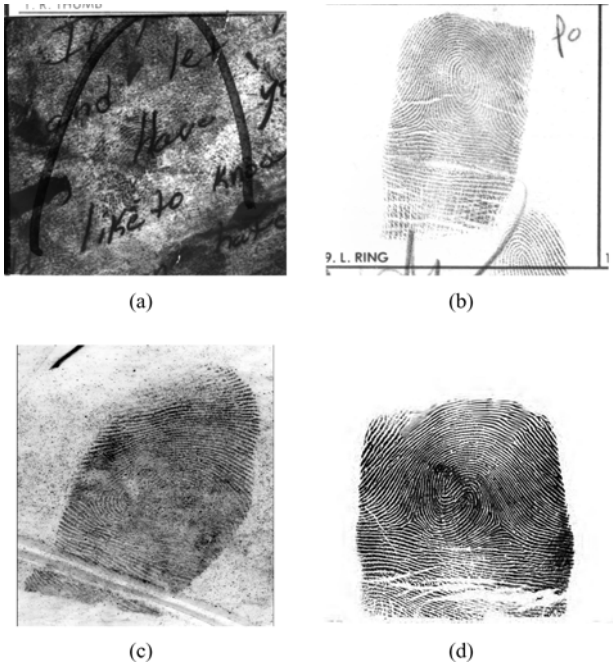

Fig. 7. Sample latent images from (a) NIST SD27 and (c) WVU latent databases. Their mated exemplars are shown in (b) and (d), respectively.

The ridge continuity map R_{cont} is then computed as:

$$R_{cont}[p,q] = \sum_{[p*,q*\in N]} \max\{I_{fc}(w_1(p,q), w_1(p*,q*)), I_{fc}(w_2(p,q), w_2(p*,q*))\}. \quad (28)$$

4) *Ridge clarity map computation*. Finally, the ridge clarity for each block centered at $[p,q]$ can be computed by taking the product of the amplitude with the ridge continuity map as follows:

$$R_{clar}[p,q] = a_1(p,q) \times R_{cont}[p,q]. \quad (29)$$

To determine the regions within each latent image I^L which need feedback, we apply a threshold th_1 on the local ridge clarity value. Let us define an indicator random variable I_F^L for each block centered at $[p,q]$ which equals 1 for latent regions which need feedback (Fig. 6c):

$$I_F^L = \begin{cases} 1, & I^L(R_{clar}[p,q]) > th_1, \\ 0, & \text{otherwise.} \end{cases} \quad (30)$$

Similarly, to decide the regions within each exemplar I^R which can provide feedback we use a threshold th_2 on the local ridge clarity value. Let us define an indicator function I_F^R for each block centered at $[p,q]$ which takes the value 1 in exemplar regions which can provide feedback (Fig. 6f):

$$I_F^R = \begin{cases} 1, & I^R(R_{clar}[p,q]) > th_2, \\ 0, & \text{otherwise.} \end{cases} \quad (31)$$

The thresholds th_1 and th_2 are empirically set to 0.1 and 0.9 respectively.

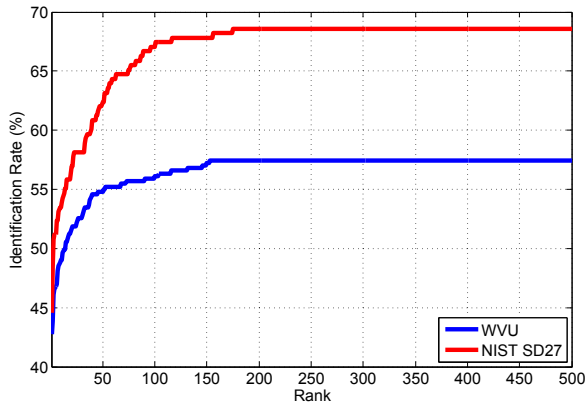

Fig. 8. Performance of the baseline latent matcher on the two latent databases against a background database of 100,000 exemplars.

5 Experimental Evaluation

5.1 Databases

The proposed feedback paradigm was evaluated on two different latent fingerprint databases, NIST SD27 [24] and WVU [25]. To increase the size of the background database, we included 27,000 rolled fingerprint images from NIST SD14 [34] database and 68,002 rolled images provided by the Michigan State Police. So, the background database consisted of 100,000 rolled fingerprints.

5.1.1 NIST SD 27

NIST SD27 database contains 258 latent images as well as their corresponding exemplar images from operational cases. The latent images in NIST SD27 have good contrast but contain complex background noise (Fig. 7a). The resolution of each image is 500 ppi.

5.1.2 WVU

The WVU database was collected in a laboratory environment at West Virginia University. It includes 449 latent images and 4,740 exemplar images out of which 449 exemplars are the true mates of the latents. The original resolution of each fingerprint image in the WVU database is 1000ppi but it was downsampled to 500ppi for our experiments. The latent images in this database have relatively clean background, but poor image contrast as compared to latents in NIST SD27 (Fig. 7c).

5.2 Size of the Candidate List (K)

One of the critical parameters while applying the paradigm is the length of the candidate list K. While choosing a large value of K would improve the odds of the mated exemplar being retrieved in the candidate list, it would also take more time to resort the candidate list. To find the optimal value of K, we plot the cumulative match characteristic (CMC) curves of the baseline matchers used in our experiments (Fig. 8). We can see that the performance gain stabilizes by rank 200. So, to optimize both accuracy and speed, the value of K is set to 200.

TABLE 1
The Total Number of Latents Where (a) Feedback Is Applied, (b) Feedback Is Applied When It Is Not Needed (Mated Examplar Retrieved at Rank-1 by the Baseline Matcher), and (c) Feedback Is Not Applied When It Could Have Been Useful (Mated Exemplar Returned amongst the Top 200 Candidates But Not at Rank-1 by the Baseline Matcher) Based on the Global Criterion for Feedback

Database	# Latents for which feedback applied	# Latents where feedback applied but not needed	# Latents where feedback not applied but needed
NIST SD27 (258 latents)	172	1	1
WVU (449 latents)	254	12	0

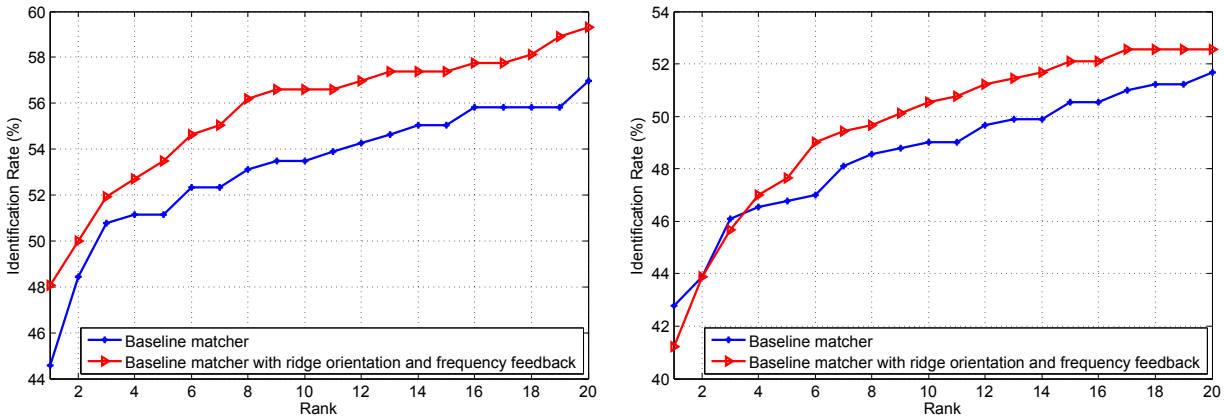

Fig. 9. Performance of the baseline matcher with and without ridge orientation and frequency feedback on (a) NIST SD27 and (b) WVU latent database (against a background database of 100,000 exemplars).

5.3 Effectiveness of the Global Criterion for Feedback

Applying feedback to a latent when it is not needed adds computational complexity without improving the accuracy. The global criterion for feedback obviates the need for feedback in about 86 out of 258 latent queries for the NIST SD27 database and in about 195 out of 449 cases for the WVU database. Table 1 lists the number of latent queries for which (i) feedback is applied even when the mated exemplar is retrieved at rank-1 by the baseline matcher [14], and (ii) feedback is not applied when the mated exemplar is not retrieved at rank-1 (but is amongst the top 200 candidates returned by the baseline matcher [14]). The low number of such cases demonstrate the efficacy of the proposed criterion in determining the need for feedback.

5.4 Performance on NIST SD27 Database

The cumulative match characteristics curves shown in Fig. 9a illustrate the performance of the baseline matcher [14] with and without feedback on the NIST SD27 database. Using the proposed ridge orientation and frequency feedback to refine the latent features improves the rank-1 identification accuracy improves by around 3.5 percent. Consistent accuracy improvement for all ranks is also observed. Figs. 10 and 11 show two latents for which the retrieval rank of the mated print is improved by applying ridge orientation and frequency feedback for the latent matcher in [14].

5.5 Performance on WVU Database

The cumulative match characteristics curves (Fig. 9b) for the WVU database also demonstrate the advantage of using the

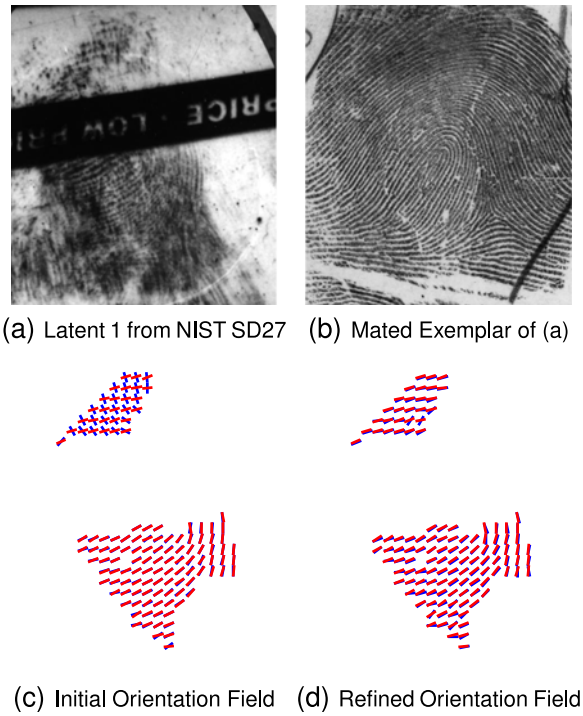

Fig. 10. Successful latent feature refinement via feedback for a latent in the NIST SD27 database. Shown in red is the exemplar orientation field and in blue is the initial and refined orientation field in (c) and (d), respectively. The rank of the mated exemplar of the latent in (a) improved from 49 to 16 amongst the 200 candidate exemplars returned by the baseline matcher after feedback.

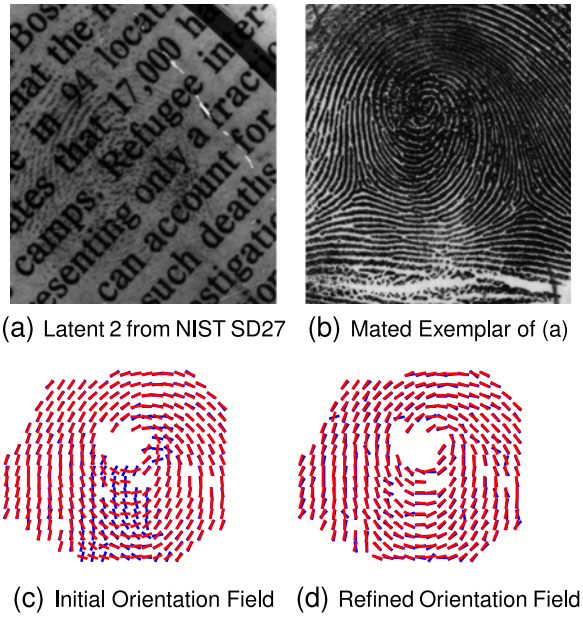

(a) Latent 2 from NIST SD27 (b) Mated Exemplar of (a)

(c) Initial Orientation Field (d) Refined Orientation Field

Fig. 11. Successful latent feature refinement via feedback for a latent in the NIST SD27 database. Shown in red is the exemplar orientation field and in blue is the initial and refined orientation field in (c) and (d), respectively. The rank of the mated exemplar of the latent (a) improved from 20 to 8 amongst the 200 candidate exemplars returned by the baseline matcher after feedback.

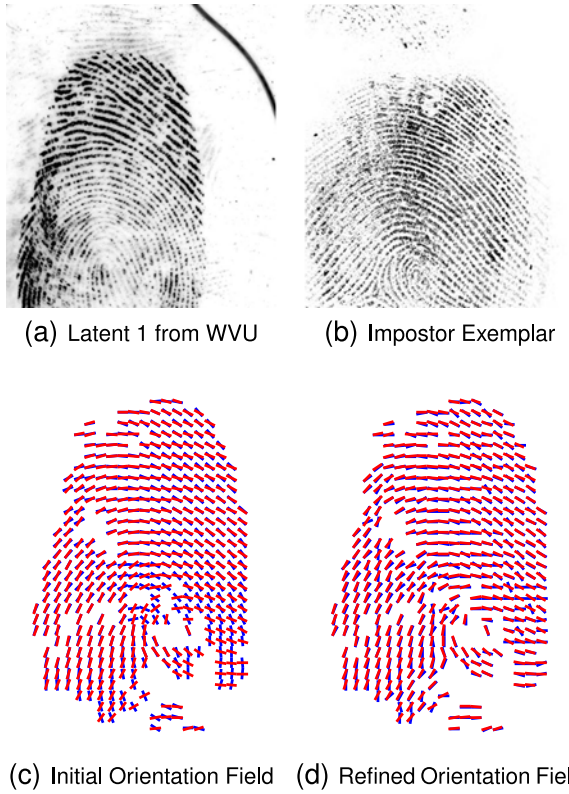

(a) Latent 1 from WVU (b) Impostor Exemplar

(c) Initial Orientation Field (d) Refined Orientation Field

Fig. 12. Failure of feedback for a latent in the WVU database. Shown in red is the exemplar orientation field and in blue is the initial and refined orientation field in (c) and (d), respectively. The retrieval rank of the mated exemplar degraded from 16 to 49 amongst the 200 candidate exemplars returned by the baseline matcher after feedback.

proposed feedback framework with the baseline matcher. Although there is a marginal decrease in the rank-1 identification accuracy, it is offset by the performance improvement of about 1-1.5 percent for the higher ranks. Note that the improvement is smaller as compared to NIST SD27 because the contrast of latents in WVU is, in general, poor making it difficult to extract level one features in the frequency domain. Fig. 12 shows an example where the retrieval rank of the mated print degrades after feedback for a latent.

The matching performance generally degrades when (i) the ridge structure of the impostor is similar to latent and (ii) the impostor exemplar is of better quality as compared to the true mate resulting in better quality features being extracted from the impostor.

5.6 Computational Complexity

The current implementation of the feedback paradigm uses local ridge orientation and ridge frequency features extracted at multiple peak points in the frequency representation of the latent image. To reduce the computational complexity, these features are computed only once for each query, and then used in matching against all exemplar candidates. Since the feedback mechanism does not involve the entire exemplar database but is used only to re-rank the top K candidates returned by the baseline matcher, the algorithmic complexity of the algorithm is $O(K)$.

The algorithm has been implemented in MATLAB and runs on a desktop system with Intel Core 2 Duo CPU of 2.93 GHz and 4.00 GB of RAM with Windows 7 Operating system. For the NIST SD27 database, the average time to extract local orientation and frequency features for a latent is about 0.74 sec and the average time to match a latent against the top 200 candidates is about 4 sec. The extra computational cost incurred in matching the latent is worth the improvement in performance, especially in forensic applications which demand high latent matching accuracy.

6 Conclusions and Future Work

Given the relatively poor quality of operational latent fingerprint images, feature extraction is one of the major challenges for a latent matching system. To deal with complex background noise in the latent, we propose incorporating feedback from exemplar (rolled or plain fingerprint) to refine feature extraction in latent with the eventual goal of improving the latent matching accuracy. We devise a method to use information in exemplar for refining the latent features (ridge orientation and frequency) and then develop a feedback paradigm to use the refined latent features to resort the candidate list returned by a latent matcher. Experimental results show good improvement in the latent matching accuracy using the feedback mechanism. We also propose a global criterion to decide if feedback is needed for a latent query. A local quality based criterion is used to determine the regions in latent where it should be applied if needed and to identify reliable regions in exemplar for providing feedback.

In future, we will explore incorporating level-2 fingerprint features such as ridge skeleton and minutiae into the feedback paradigm to further improve latent matching accuracy.

ACKNOWLEDGMENTS

This material was based upon work supported by the National Science Foundation under Grant No. 1066197. Eryun Liu's research was partially supported by the National Natural Science Foundation of China under Grant No. 61100234. The authors would like to thank Prof. Jianjiang Feng of Tsinghua University, China, and Soweon Yoon of Michigan State University for providing useful feedback during the course of this research. An earlier version of this paper appeared in the proceedings of the 6th IAPR International Conference on Biometrics (ICB), 2013 [35].

REFERENCES

[1] F. Galton, *Finger Prints*. New York, NY, USA: MacMillan, 1892.
[2] C. Champod, C. Lennard, P. Margot, and M. Stoilovic, *Fingerprints and Other Ridge Skin Impressions*. Boca Raton, FL, USA: CRC Press, 2004.
[3] Integrated automated fingerprint identification system (IAFIS) [Online]. Available: http://www.fbi.gov/about-us/cjis/fingerprints_biometrics/iafis
[4] H. Lee and R. Gaensslen, *Advances in Fingerprint Technology*. Boca Raton, FL, USA: CRC Press, 2001.
[5] C. Wilson. (2004). Fingerprint vendor technology evaluation 2003: Summary of results and analysis report, nistir 7123 [Online]. Available: http://fpvte.nist.gov/report/ir_7123_analysis.pdf
[6] (2007). Evaluation of latent fingerprint technologies [Online]. Available: http://fingerprint.nist.gov/latent/elft07/
[7] NIST, Summary of results from ELFT07 phase i testing (2007). [Online]. Available: http://fingerprint.nist.gov/latent/elft07/phase1_aggregate.pdf
[8] M. Indovina, V. Dvornychenko, R. Hicklin, and G. Kiebuzinski, ELFT-EFS evaluation of latent fingerprint technologies: Extended feature sets [evaluation# 2]. (2012). [Online]. Available: http://biometrics.nist.gov/cs_links/latent/elft-efs/NISTIR_7859.pdf
[9] FBI, Next generation identification. (2012) [Online]. Available: http://www.fbi.gov/about-us/cjis/fingerprints_biometrics/ngi
[10] D. Ashbaugh, *Quantitative-Qualitative Friction Ridge Analysis: An Introduction to Basic and Advanced Ridgeology*. Boca Raton, FL, USA: CRC Press, 1999.
[11] A. Jain and J. Feng, "Latent fingerprint matching," *IEEE Trans. Pattern Anal. Mach. Intell.*, vol. 33, no. 1, pp. 88–100, Jan. 2011.
[12] J. Feng, J. Zhou, and A. Jain, "Orientation field estimation for latent fingerprint enhancement," *IEEE Trans. Pattern Anal. Mach. Intell.*, vol. 35, no. 4, pp. 925–940, Apr. 2013.
[13] S. Yoon, J. Feng, and A. Jain, "On latent fingerprint enhancement," in *Proc. SPIE Conf. Series*, 2010, vol. 7667, pp. 766 707_01–766 707_10.
[14] A. Paulino, J. Feng, and A. Jain, "Latent fingerprint matching using descriptor-based hough transform," *IEEE Trans. Inf. Forensics Security*, vol. 8, no. 1, pp. 31–45, Jan. 2013.
[15] R. Duda, P. Hart, and D. Stork, *Pattern Classification*, 2nd ed. New York, NY, USA: Wiley, 2001.
[16] B. Coppin, *Artificial Intelligence Illuminated*. Boston, MA, USA: Jones & Bartlett, 2004.
[17] H. Choi, M. Boaventura, I. Boaventura, and A. Jain, "Automatic segmentation of latent fingerprints," in *Proc. IEEE Fifth Int. Conf. Biometrics: Theory, Appl. Syst.*, pp. 303–310, 2012.
[18] J. Hollands and C. Wickens, *Engineering Psychology and Human Performance*. Englewood Cliffs, NJ, USA: Prentice Hall, 1999.
[19] N. Oliver, B. Rosario, and A. Pentland, "A Bayesian computer vision system for modeling human interactions," *IEEE Trans. Pattern Anal. Mach. Intell.*, vol. 22, no. 8, pp. 831–843, Aug. 2000.
[20] A. Oliva, A. Torralba, M. Castelhano, and J. Henderson, "Top-down control of visual attention in object detection," in *Proc. IEEE Int. Conf. Image Process.*, 2003, vol. 1, pp. I–253.
[21] E. Borenstein and S. Ullman, "Combined top-down/bottom-up segmentation," *IEEE Trans. Pattern Anal. Mach. Intell.*, vol. 30, no. 12, pp. 2109–2125, Dec. 2008.
[22] M. Bodén, "A guide to recurrent neural networks and backpropagation," *DALLAS Project. Rep. NUTEK-Supported Project AIS-8, SICS. Holst: Appl. Data Anal. Learn. Syst.*, no. 2, pp. 1–10, 2001.
[23] I. Dror, A. Peron, S. Hind, and D. Charlton, "When emotions get the better of us: The effect of contextual top-down processing on matching fingerprints," *Appl. Cognitive Psychol.*, vol. 19, no. 6, pp. 799–809, 2005.
[24] NIST Special Database 27 [Online]. Available: http://www.nist.gov/srd/nistsd27.cfm
[25] West Virginia University (WVU) latent fingerprint database [Online]. Available: http://www.cse.msu.edu/~rossarun/
[26] A. Jain and J. Feng, "Latent palmprint matching," *IEEE Trans. Pattern Anal. Mach. Intell.*, vol. 31, no. 6, pp. 1032–1047, Jun. 2009.
[27] A. Jain, K. Nandakumar, and A. Ross, "Score normalization in multimodal biometric systems," *Pattern Recognit.*, vol. 38, no. 12, pp. 2270–2285, Dec. 2005.
[28] H. O. Lancaster and E. Seneta, *Chi-Square Distribution*. New York, NY, USA: Wiley, 1969.
[29] S. Lalitha and N. Kumar, "Multiple outlier test for upper outliers in an exponential sample," *J. Appl. Statist.*, vol. 39, no. 6, pp. 1323–1330, 2012.
[30] G. Casella and R. L. Berger, *Statistical Inference*, vol. 70. Belmont, CA, USA: Duxbury Press, 1990.
[31] T. Lewis and N. Fieller, "A recursive algorithm for null distributions for outliers: I. gamma samples," *Technometrics*, vol. 21, no. 3, pp. 371–376, 1979.
[32] S. Yoon, E. Liu, and A. K. Jain, "On latent fingerprint image quality," Presented at the Int. Workshop Computational Forensics, Tsukuba, Japan, 2012.
[33] H. Fronthaler, K. Kollreider, and J. Bigun, "Local features for enhancement and minutiae extraction in fingerprints," *IEEE Trans. Image Process.*, vol. 17, no. 3, pp. 354–363, Mar. 2008.
[34] NIST Special Database 14 [Online]. Available: http://www.nist.gov/srd/nistsd14.cfm
[35] E. Liu, S. S. Arora, K. Cao, and A. K. Jain, "A feedback paradigm for latent fingerprint matching," *in Proc. 6th Int. Conf. Biometrics (ICB '13)*, 2013.

Sunpreet S. Arora received the Bachelor of Technology (Hons.) degree in computer science from the Indraprastha Institute of Information Technology, Delhi (IIIT-D), in 2012. He is currently a doctoral student at the Department of Computer Science and Engineering, Michigan State University. His research interests include biometrics, pattern recognition, and computer vision. He received the prestigious National Talent Search (NTS) scholarship by the National Council of Educational Research and Training (NCERT), India, in 2006. He received the Best Poster Award at the IEEE Fifth International Conference on Biometrics: Theory, Applications and Systems (BTAS), 2012. He is a student member of the IEEE.

Eryun Liu received the bachelor's degree in electronic information science and technology and the PhD degree in pattern recognition and intelligence system from Xidian University, Xian, Shaanxi China, in 2006 and 2011, respectively. He was affiliated with Xidian University as an assistant professor from 2011 to 2013. He was a postdoctoral fellow at the Department of Computer Science & Engineering, Michigan State University, East Lansing. He is currently affiliated with the Department of Information Science & Electronic Engineering, Zhejiang University, Hangzhou, China, as an assistant professor. His research interests include biometric recognition, point pattern matching and information retrieval, with a focus on fingerprint and palmprint recognition. He is a member of the IEEE.

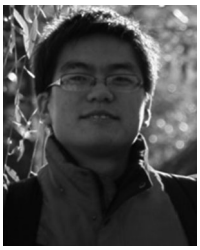

Kai Cao received the PhD degree from Key Laboratory of Complex Systems and Intelligence Science, Institute of Automation, Chinese Academy of Sciences, Beijing, China, in 2010. He is currently a postdoctoral fellow at the Department of Computer Science & Engineering, Michigan State University, East Lansing. He is also with Xidian University as an associate professor. His research interests include biometric recognition, image processing and machine learning.

Anil K. Jain is a University distinguished professor at the Department of Computer Science and Engineering, Michigan State University. His research interests include pattern recognition and biometric authentication. He served as the editor-in-chief of the *IEEE Transactions on Pattern Analysis and Machine Intelligence* (1991-1994). The holder of eight patents, he is the author of a number of books, including *Handbook of Fingerprint Recognition* (2009), *Handbook of Biometrics* (2011), *Handbook of Multibiometrics* (2006), *Handbook of Face Recognition* (2005), *BIOMETRICS: Personal Identification in Networked Society* (1999), and *Algorithms for Clustering Data* (1988). He served as a member of the Defense Science Board and The National Academies committees on Whither Biometrics and Improvised Explosive Devices. He received the 1996 IEEE Transactions on Neural Networks Outstanding Paper Award and the Pattern Recognition Society best paper awards in 1987, 1991, and 2005. He has received Fulbright, Guggenheim, Alexander von Humboldt, IEEE Computer Society Technical Achievement, IEEE Wallace McDowell, ICDM Research Contributions, and IAPR KingSun Fu Awards. He is a fellow of the AAAS, ACM, IAPR, IEEE, and SPIE.